Ultrafast Electronic and Vibrational Energy Relaxation of Fe(acetylacetonate)$_3$ in Solution

Ermelinda M. S. Maçôas, Robertas Kananavicius, Pasi Myllyperkiö, Mika Pettersson, and Henrik Kunttu*

Nanoscience Center, Department of Chemistry, P.O. Box 35, FI-40014 University of Jyväskylä, Finland

Received: September 25, 2006; In Final Form: January 4, 2007

Transient mid-infrared spectroscopy is used to probe the dynamics initiated by excitation of ligand-to-metal (400 nm) and metal-to-ligand (345 nm) charge transfer states of Fe^{III} complexed with acetylacetonate (Fe(acac)$_3$, where acac stands for deprotonated anion of acetylacetone) in solution. Transient spectra in the 1500−1600 cm^{-1} range show two broad absorptions red-shifted from the bleach of the ν(CO) ($\approx$1575 cm^{-1}) and ν(C═C) ($\approx$1525 cm^{-1}) ground state absorptions. Bleach recovery kinetics has a time constant of 12−19 ps in chloroform and tetrachloroethylene and it decreases by 30−40% in a 10% mixture of methanol in tetrachloroethylene. The transient absorptions experience band narrowing simultaneously with blue-shifting of the absorption maxima. Both phenomena have time constants of 3−9 ps with no evident dependence on the solvent. The experimental observations are ascribed to fast conversion of the initially excited charge transfer states to the ligand field manifold, and subsequent vibrational cooling on the lowest ligand field excited state prior to electronic conversion to the ground state. The analysis of time dependent bandwidths and positions of the transient absorptions provides some evidence of mode specific vibrational cooling.

Introduction

Understanding the most elementary steps of chemical reactions, and in particular the microscopic mechanisms dictating their time scales, remains the central topic in condensed phase chemistry and dynamics.[1] Such processes are often characterized by ultrafast timescales of picoseconds or below, and the complex chemical events are not determined solely by the intramolecular potential energy surfaces.[2] Instead, the surrounding solvent plays a crucial role in all dynamics, and thus increases the dimension of the problem. A variety of time-resolved techniques based on ultrashort laser pulses are currently available and have been routinely used for real time monitoring of chemical events.[3,4] In most cases, transient phenomena triggered by the initial excitation pulse have been followed by time-resolved electron spectroscopy. For systems possessing large oscillator strengths at desired frequencies, this approach provides a means to transient spectroscopy with very high sensitivity. However, the large bandwidths of the electronic transitions complicate the analysis and, in many cases, some of the chemically interesting structural information cannot be extracted from the experiment.

Ultrafast infrared spectroscopy is particularly suitable for tackling problems in which nuclear motion, i.e., chemical change, vibrational dynamics, solute−solvent energy transfer, etc., is of concern.[5] In this technique, as it is mostly applied today, the spectral bandwidth (typically 150−200 cm^{-1}) of the ultrashort mid-infrared pulse is used as a dispersed source to probe time dependent changes in molecular vibrations after the visible, ultraviolet (UV), or IR pump pulse.[5−12] These changes can be related to absorption intensities, bandwidths, or band positions, all providing valuable information of the dynamic system.[6] Moreover, the vibrational bands of molecules are relatively narrow, enabling simultaneous monitoring of several vibrations in the same spectral window defined by the IR pulse properties and the detection system. As demonstrated in a number of previous studies, combining a multi-element IR array detector with an ultrafast IR source provides an extremely versatile tool for time-resolved studies of various processes.[10−15] However, the applicability of IR probing obviously suffers from the fact that infrared transitions are often relatively weak, and strong pump intensities and high molecular concentrations are essential for transient measurements. Nevertheless, as a structurally resolving technique with ultrafast time resolution, time-resolved IR spectroscopy provides such insights into chemical reactivity and relaxation, which are not obtainable with any other method.

The recent review article by Nibbering and co-workers provides an excellent source for the current status of activities in interrogation of structural dynamics by time-resolved vibrational spectroscopy.[5] One of the focus areas addressed by several research groups is ultrafast dynamics of transition metal complexes, which are particularly suitable for the visible/UV pump−IR probe approach.[6−18] Moreover, these conceptually simple systems possess interesting light-induced ligand exchange reactions, which have been studied in great detail. The recent investigations by the Harris group on ligand arrangement reactions of Cr(CO)$_6$ in alcohols of variable chain lengths, provide an example of the state-of-the-art to which the field has evolved.[15] Interestingly, the obtained results serve as important steps toward understanding of dynamics of molecular recognition processes.

We have recently acquired a time-resolved IR setup based on ultrashort IR pulses with a spectral width of 200 cm^{-1} and a 2 × 64 element mercury cadmium telluride (MCT) array detector for their frequency dispersed detection at adjustable time delay relative to a visible or UV trigger pulse. Fe(acac)$_3$ (for structure, see Figure 1) was chosen as a target in our first time-resolved IR studies because it possesses strong visible and UV absorptions suitable for excitation as well as two intense vibrational modes of different nature suitable for IR probing.

* Corresponding author. E-mail: Henrik.Kunttu@jyu.fi.

10.1021/jp066271z CCC: $37.00
Published on Web 02/13/2007

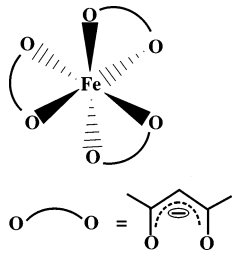

Figure 1. Structure of Fe(acac)$_3$.

This investigation is expected to reveal relevant information about the structure of excited states involved in the dynamics.

Fe(acac)$_3$ is subject to solvolysis in protic coordinating solvents such as alcohols but is, due to the negatively charged ligand, nonreactive in aprotic solvents.[19] Indeed, this property distinguishes Fe(acac)$_3$ from photoreactive transition metal carbonyls and their derivatives, and thus limits the dynamics to electronic conversion and vibrational relaxation processes, involving the solvent as a thermal bath accepting the excess energy introduced in the system. Fast vibrational energy relaxation (VER) can be expected on the basis of the high vibrational state density of Fe(acac)$_3$ (123 vibrational degrees of freedom).

In this paper the UV pump−IR probe spectroscopy is used to follow the bleach of the ground electronic state absorptions associated with the CO and C═C stretching modes (ν(CO), $\approx$1575 cm^{-1}; ν(CC), $\approx$1525 cm^{-1}),[20] as well as the time evolution of the absorption transients observed in the 1620−1480 cm^{-1} region. The present investigation is closely connected to the previous UV pump−IR probe studies on Rh(CO)$_2$(acac),[6] and the visible/UV pump−visible probe studies of the very related compound, Cr(acac)$_3$.[21]

Experimental Section

Fe(acac)$_3$ was synthesized according to the procedure by Dunne and Cotton,[22] and 20 mM solutions were prepared in chloroform, tetrachloroethylene ,and 10% methanol/tetrachloroethylene mixture. A closed-cycle flow cell with CaF_2 windows was used to circulate the solution and ensure complete exchange of sample for measurements at 1 kHz repetition rate.[23] The optical path of the cell was fixed to 100 μm.

The laser and detection setup (UV/vis pump−mid-IR probe spectrometer) is based on a Ti:sapphire oscillator (Coherent, Mira 900) and a multipass amplifier (Quantronics, Odin) providing 800 nm pulses with 100 fs duration and 0.8 mJ energy at a 1 kHz rate. Tunable mid-IR pulses are generated by a two stage optical parametric amplifier (OPA), based on a β-barium borate (BBO) crystal, used in combination with difference frequency mixing in a $AgGaS_2$ crystal. In the following, we briefly describe the mid-IR source, and setup for transient IR spectroscopy. More details can be found in ref 24.

A single filament white light continuum, generated in a 1 mm sapphire plate is used as a seed for a 4 mm type II BBO crystal in the first amplification stage. Pump beams are aimed into the seed direction by dichroic mirrors, which are reflecting 800 nm p-polarization, while being transparent for signal s-polarization (1200−1620) nm and idler p-polarization (1520−2500) nm. The first pass pump beam (800 nm 3 μJ) is tightly focused onto the crystal by a 50 cm lens. To generate an amplified beam of good spatial quality, the pump beam waist is much smaller than that of the seed. The signal and idler parts of the amplified near-infrared radiation are separated from each other with a dichroic mirror, and the signal is focused back to the crystal for a second amplification stage pumped with 400 μJ pulses at 800 nm. The beam waist of the pump is reduced to $\sim$1.5 mm by a 1:4 telescope to simultaneously carefully collimate the beam. A filter is used to block all visible radiation. The energy of signal and idler after the second pass is approximately 80 μJ, which corresponds to an energy conversion efficiency of 20%. In the final stage, signal and idler are separated by a second dichroic mirror, and focused with gold plated spherical mirrors onto a 1.5 mm $AgGaS_2$ crystal (φ = 45° Θ = 40°), in which difference frequency is generated. The time overlap of the beams is ensured by bringing one of them through a variable delay line. A long pass (>2.5 m) filter is used to block signal and idler after the crystal. This setup generates tunable mid-IR pulses in the 3−7 μm range, with an energy of 1−4 μJ and a spectral width of $\sim$200 cm^{-1}.

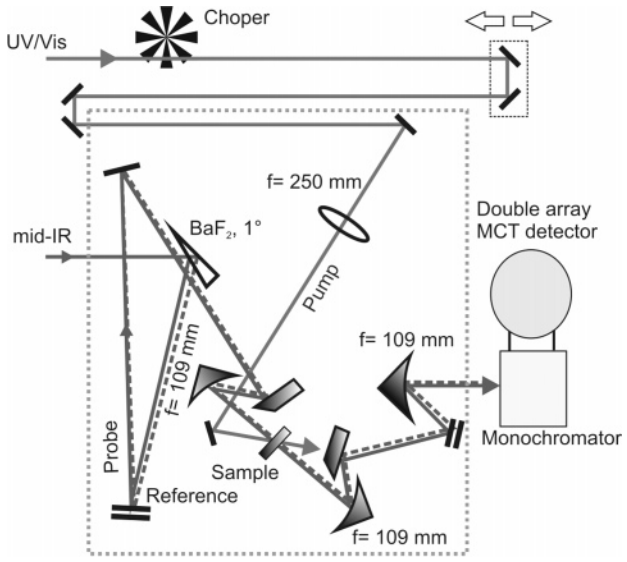

Figure 2. Schematics of the IR spectrometer used in the transient UV/vis pump−mid-IR probe measurements.

Figure 2 shows the setup used for the transient IR measurements. The IR beam is separated into probe and reference beams by reflecting a small fraction of the beam by a BaF_2 1° wedge. The two beams are then separated in a vertical plane, reflected by independent mirrors, and focused to separate spots in the sample by a parabolic off-axis 30° gold plated mirror. After the sample, the beams are collimated by a second parabolic mirror and focused onto the slit of the spectrograph using two independent alignment mirrors and a third parabolic mirror. Finally, the IR beams are dispersed in a spectrograph (Acton Research Corp., f = 150 mm, 150 grooves/mm grating) and detected with a 2 × 64 channel double array HgCdTe detector (Infrared Systems Development). The spectral resolution of detection is 1.3 cm^{-1}/pixel. The UV pump and IR probe beams are focused to the same spot on the sample. A synchronized chopper blocks every second pump pulse, and the transient signal is obtained by comparing probe and reference signals with and without UV excitation. Typically, data from three independent scans were averaged before analysis. The time resolution is estimated to be $\sim$400 fs by monitoring the rise time of electronic absorption in a thin Si film.

The 400 nm pulses (1−2 μJ) are simply obtained by second harmonic generation in a 1 mm thick BBO crystal and guided to the sample through a computer controlled delay line. The UV pulses (345 nm, 0.8 μJ) are generated by sum frequency mixing the output from a two stage NOPA with the fundamental laser radiation (800 nm) in a 1 mm thick BBO crystal.

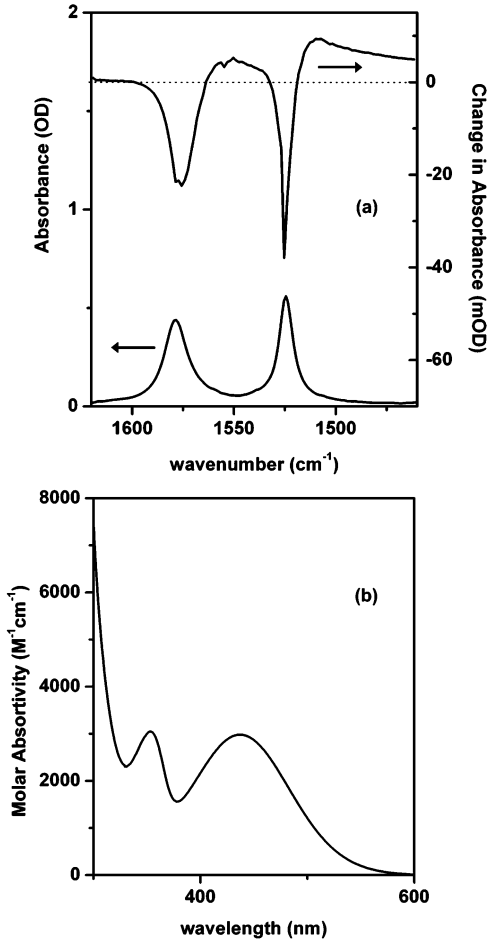

Figure 3. Steady state IR (a) and UV−vis (b) absorption spectra of a 20 mM solution of $Fe(acac)_3$ in TCE. The transient IR absorption spectrum recorded immediately after 400 nm excitation is shown in the top trace of plot (a).

Results

Transient IR measurements of $Fe(acac)_3$ were carried out in tetrachloroethylene (TCE) and chloroform at 20 mM concentration. The transparency of TCE in the 1500−1600 cm^{-1} range allows clean spectral observations of the strong ν(CO) and ν(C═C) features as well as line shape analysis of the transient absorptions detected in this region (see Figure 3). On the other hand, the absorption of chloroform overlaps partially with the ν(C═C) band, preventing a reliable line shape analysis of the transient signals. Nevertheless, the ground state bleach kinetics of these two strong absorptions could be obtained with confidence in both solutions. Additionally, to investigate whether $Fe(acac)_3$ is subject to photoinduced ligand exchange with the solvent, experiments were carried out in a binary TCE/methanol mixture containing 10% methanol. The reduced methanol concentration was essential for transparency of the sample in the studied spectral region.

As shown in Figure 3, $Fe(acac)_3$ possesses strong electronic absorptions in the 300−600 nm spectral region. The individual bands near 270, 350, and 440 nm have been assigned to ligand $\pi-\pi^*$, metal-to-ligand charge transfer (MLCT), and ligand-to-metal charge transfer (LMCT) transitions, respectively.[25] In this investigation, excitation wavelengths 345 and 400 nm were used to initiate dynamics.

The overall time dependent spectral changes induced by 400 nm excitation are shown as a contour plot in Figure 4. It can be seen that the two intense ground state vibrations are strongly

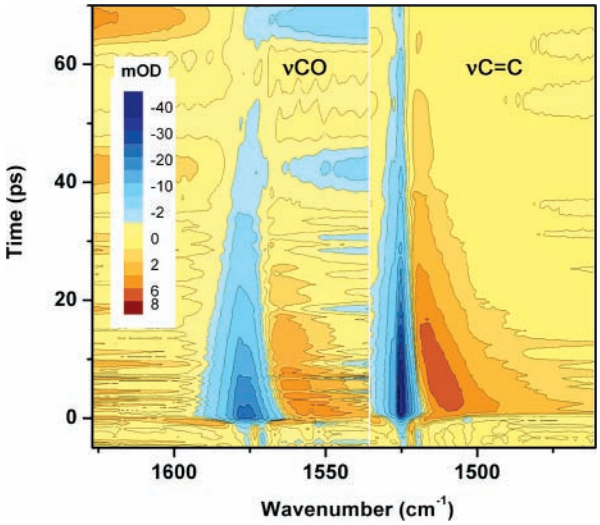

Figure 4. Contour plot of the transient spectra of $Fe(acac)_3$ in TCE after excitation at 400 nm.

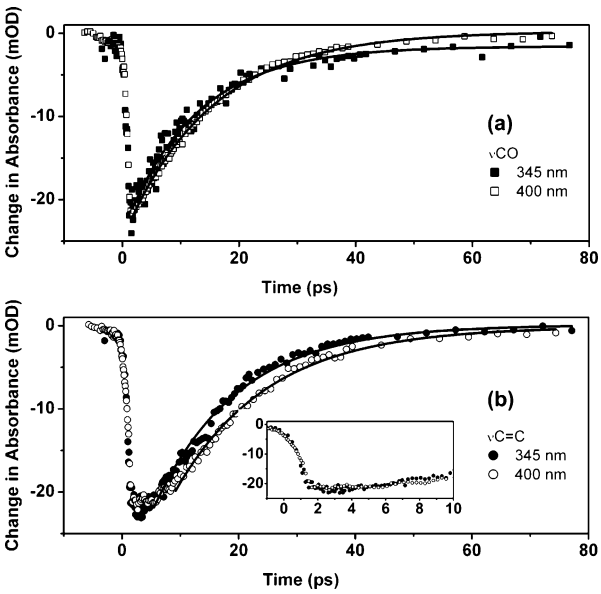

Figure 5. Bleach decay kinetics of the ν(CO) (a) (1578 cm^{-1}) and ν(C═C) (b) (1524 cm^{-1}) vibrational modes of $Fe(acac)_3$ in TCE observed after excitation at 400 and 345 nm. The solid lines are fits to one exponential rise function. The insert in (b) shows the flattening of the data at early times (see discussion in the text).

(20−40 mOD) bleached at zero delay between the pump and the probe (negative transients), and new bands grow transiently (positive signals) on the low-frequency side of the bleached bands (see also Figure 3). Furthermore, the bleached absorptions recover completely within some tens of picoseconds, and before that the positive bands narrow and their maxima are blue-shifted. At longer delay times the spectrum fully recovers its initial structure with no evidence of formation of stable photoproducs. In the following these observations are presented in more detail.

Figure 5 shows recovery kinetics of the bleached ν(CO) and ν(C═C) bands of the electronic ground state of $Fe(acac)_3$ in TCE solution following 345 and 400 nm excitation. For the ν(CO) band, the bleach of absorption appears instantaneously after the excitation pulse, and maximum bleach of ∼22 mOD is formed within 1 ps. Due to the well separated rise and decay times, the bleach recovery of this band is well fitted with a single-exponential function with a characteristic time constant

TABLE 1: Kinetic Parameters for Recovery of the ν(CO) and ν(C═C) Bands of Fe(acac)$_3$ after Initial Bleach at 345 and 400 nm Excitation[a]

	τ (ps), 345 nm excitation		τ (ps), 400 nm excitation	
solvent	ν(C═C)	ν(CO)	ν(C═C)	ν(CO)
chloroform	*b*	*b*	18.7 ± 0.8	14.0 ± 2.0
TCE	14.4 ± 0.5	12.4 ± 0.8	17.0 ± 0.6	15.0 ± 0.2
TCE + 10% MeOH	10.4 ± 0.3	8.2 ± 0.2	10.6 ± 0.3	8.4 ± 0.05

[a] The characteristic times, τ, are obtained from single-exponential fits. [b] Not measured. Spectral overlap with the solvent prevents reliable measurement.

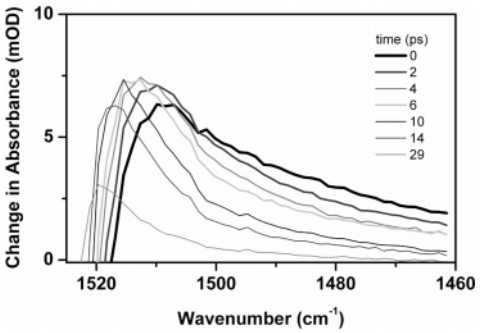

Figure 6. Narrowing and blue-shifting of the transient absorption at lower wavenumbers from the ν(C═C) vibrational mode of Fe(acac)$_3$ in TCE after 400 nm excitation.

of 8−15 ps, depending on the solvent and the excitation wavelength. As observed in Figure 5, the evolution of the ν-(C═C) absorption is somewhat different. The bleach of this band is also appearing at instrumental limited response time, but it remains apparently constant for several picoseconds before recovery of the absorption starts. Apart from this plateau in the kinetic data, the recovery of the ν(C═C) absorption proceeds with kinetics rather similar to that of the ν(CO) band. This behavior complicates the analysis of the bleach kinetics of the ν(C═C) absorption; however, its recovery can be sufficiently well fitted with a single-exponential function. Table 1 collects the parameters of the bleach kinetics for Fe(acac)$_3$/TCE, Fe-(acac)$_3$/TCE(10%MeOH), and Fe(acac)$_3$/chloroform solutions. It should be noted that the data obtained for chloroform samples is associated with a larger experimental error; however, they provide useful comparison between different solvents.

As indicated in Figures 3 and 4, the photoinduced bleach of the ν(CO) and ν(C═C) bands is accompanied by growth of new transient bands slightly red-shifted from the bleached absorptions. The transient spectral features appear instantaneously after the UV excitation and possess initially broad spectral bandwidths with fwhm (full width at half-maximum) of 20−40 cm^{-1}. In comparison, the FWHMs of the ground state absorptions are 14 and 8 cm^{-1} for the ν(CO) and ν(C═C), respectively. Interestingly, both the spectral widths and positions of the absorption maxima of the transients are strongly time dependent. Roughly, the fwhm of the absorptions narrows down to half of their initial value, and the band maxima move ∼10−15 cm^{-1} toward the bleached ground state absorption in time scales of the order of 2−10 ps. In Figure 6, a sequence of spectral traces recorded as a function of delay between the UV and IR pulses shows a typical behavior of the absorption transients. The pronounced asymmetry of the spectral envelopes, which somewhat complicates their analysis, is caused by overlap between the negative (bleach) and positive transients. To extract the fwhm and maxima of the strongly convoluted transients with confidence, the spectra were fitted with Gaussian functions as shown in Figure 7. The time evolution of the band widths and maxima as obtained from such analysis are shown for the positive transients in Figures 8 and 9, respectively.

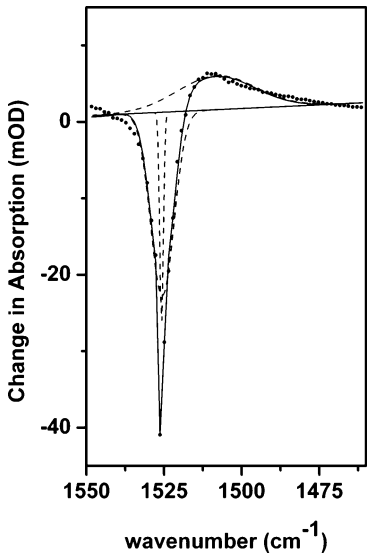

Figure 7. Deconvolution of the transient spectrum (dotted line) observed for Fe(acac)$_3$ in TCE 1 ps after 400 nm excitation. The bleach and absorption bands were fitted with two and one Gaussian function (dashed line), respectively. The result of the fit is shown as a solid line.

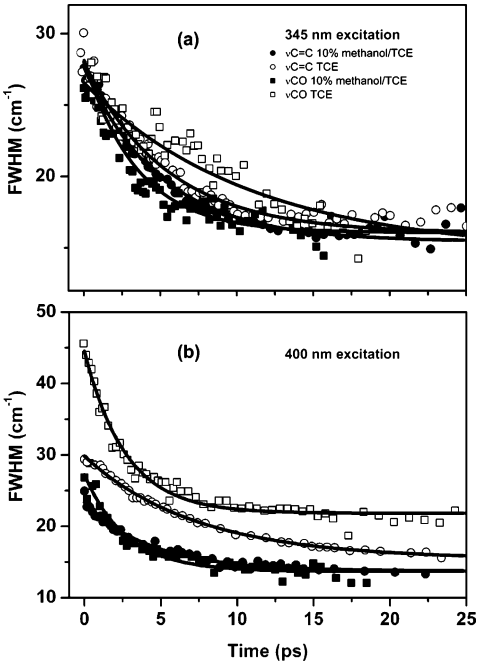

Figure 8. Time dependent narrowing of the transient absorptions appearing red-shifted from the steady state ν(CO) and ν(C═C) absorptions. Shown are the fwhm of the transients observed for Fe-(acac)$_3$ in pure TCE and in 10% methanol/TCE mixture after excitation at 345 nm (a) and 400 nm (b). The solid lines are fits to eq 1 with time constants in TCE/TCE + 10% MeOH solutions of 10.9 ± 0.7/3.8 ± 0.3 ps (ν(CO)) and 5.4 ± 0.4/5.1 ± 0.2 ps (ν(C═C)) for 345 nm excitation and 2.7 ± 0.1/2.7 ± 0.3 ps (ν(CO)) and 7.3 ± 0.3/4.4 ± 0.3 ps (ν(C═C)) for 400 nm excitation.

Discussion

The time dependent IR observations clearly indicate that, following the initial triggering pulse at 400 or 345 nm, the number of ground state Fe(acac)$_3$ molecules is transiently

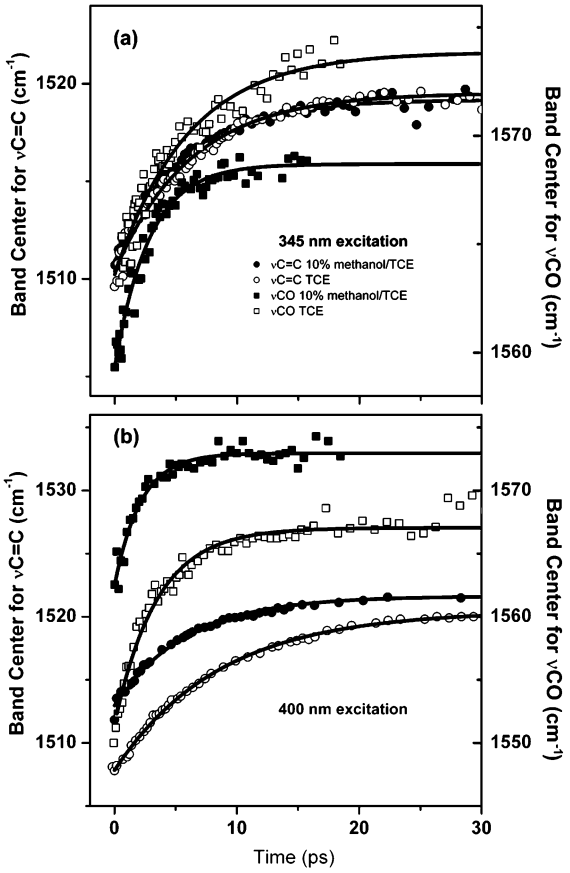

Figure 9. Time dependent blue-shifting of the transient absorptions near the steady state ν(CO) and ν(C═C) absorptions. Shown are the band centers of the transients observed for $Fe(acac)_3$ in pure TCE and in TCE + 10% MeOH mixture after excitation at 345 nm (a) and 400 nm (b). The solid lines are fits to one exponential rise functions with time constants in TCE /TCE + 10% MeOH solutions of 6.0 ± 0.4/2.8 ± 0.2 ps (ν(CO)) and 6.2 ± 0.3/5.5 ± 0.2 ps (ν(C═C)) for 345 nm excitation and 3.4 ± 0.1/2.1 ± 0.2 ps (ν(CO)) and 8.6 ± 0.1/5.9 ± 0.1 ps (ν(C═C)) for 400 nm excitation.

reduced. Equally clear is that at later times, ~60 ps after the excitation, this reduction is fully recovered excluding permanent loss channels such as ligand substitution reactions. This observation is not surprising due to the charged nature of the ligand, and the known photostability of $Fe(acac)_3$[19,26] Similar photostability upon charge transfer excitation has been reported for the chromium analogue, $Cr(acac)_3$.[21] Consistently, our attempt to enhance reactivity by adding 10% methanol in TCE failed. In a somewhat related study, Heilweil and co-workers reported photosubstitution of one of the CO ligands of $Rh(CO)_2$-(acac) in several solvents but the similar compound $Ir(CO)_2$-(acac) showed no reactivity.[6] The ground state bleach of the latter recovered in a time scale of 40 ps and was attributed to relaxation of electronic state(s) prepared by the excitation.

Bleach. All of our kinetic traces recorded for the ν(CO) bleach are well fitted with single-exponential recovery. The obtained fits indicate that the relaxation channel responsible for recovering the initial situation has a time constant of 12−19 ps in chloroform and TCE. Adding 10% methanol in TCE caused a decrease of the time constant to 8−10 ps, which corresponds to a 30−40% increase in the relaxation rate. Because the experiment monitors the recovery of the ground state population, these time scales represent total relaxation of the system, i.e., electronic and vibrational relaxation. Therefore, the dynamics of individual processes along the relaxation path, and their dependence on the solvent cannot be resolved on the basis of only kinetics of ground electronic state recovery. However, important implications arise from the analysis. Because the vibrational cooling times deduced from the analysis of the transient absorptions (see below) are significantly smaller than the bleach recovery times, we are forced to conclude that the final relaxation is limited by electronic conversion, and we thus ascribe the bleach recovery time to electronic relaxation time of this bottleneck state. There are only minor differences in the bleach recovery times recorded at the two excitation wavelengths (see Figure 5 and Table 1). Especially in 10% methanol solution the two excitation energies yield identical bleach kinetics, indicating that electronic conversion to a common bottleneck state occurs within few picoseconds. Interestingly, a recent UV/vis pump−vis probe study on $Cr(acac)_3$ showed that ISC can compete effectively with vibrational relaxation in high-energy electronic states. In this system, both ligand field ($^4A_2 \rightarrow {}^4T_2$) and charge transfer ($^4A_2 \rightarrow {}^4$LMCT) absorption leads to very rapid population of the lowest energy electronic excited state (ligand-field ^{2}E state), which then relaxes to the $^4A_2$ ground state with a characteristic time of 700 ps.[21] As discussed by several authors, the excited state evolution of metal-containing systems may be rather peculiar, and even conceptually forbidden electronic transitions can proceed with subpicosecond rates exceeding vibrational cooling rates.[21,27,28] In the present case, the complete recovery of the baseline on a much faster time scale would exclude, besides formation of any photoproducts, the existence of long-lived excited states along the relaxation pathway.

As pointed out before, the anomalous time evolution of the bleach recovery of the ν(C═C) vibration, in contrast with that of the ν(CO) mode, shows a region of constant bleach before recovery of the absorption. After careful examination of the experimental setup, and repeating the experiment several times, we are convinced that the observation is, indeed, real. Moreover, the fact that the maximum bleach occurs at positive times excludes perturbed free induction decay caused by slow vibrational dephasing as the origin for the odd behavior.[29] On the basis of these arguments, the observed plateau is ascribed to time dependent spectral overlap between the negative absorption (bleach) and the dynamically evolving positive transient band on its low-frequency side. Note that consistently with the ν(CO) bleach, also the ν(C═C) bleach exhibits an apparent increase in the recovery rate in the TCE + 10% methanol solvent (≈10 ps) with respect to the other two solvents tested (14−19 ps).

Absorption. In the following, the time dependence of the transient absorptions red-shifted from the vibrationally relaxed ground electronic state ν(CO) and ν(C═C) bands is discussed. As shown in Figures 8 and 9, the band maxima and fwhm of the transient absorptions are strongly time dependent in all solvents and both excitation wavelengths. This is, in fact, well-known behavior of vibrationally hot molecules.,[6,7,9,10] for which narrowing of the initially broad spectral envelopes is a signature of vibrational cooling, i.e., dissipation of the vibrational excitation to the solvent. Therefore, the transient absorptions belong to the ν(CO) and ν(C═C) modes of either the ground or excited electronic states that are vibrationally excited. The temporal behavior of the bandwidth provides information concerning the rate of vibrational cooling via the formula suggested by Heilweil et al.:[6]

$$\mathrm{fwhm}(t) = [(A \exp^{-t/\tau} + \Gamma)^2 + (\mathrm{IRF})^2]^{1/2} \qquad (1)$$

where Γ is the final value of the bandwidth at equilibrium (excluding instrumental resolution), A is the additional width

TABLE 2: Characteristic Vibrational Cooling Times, τ, of ν(C═C) and ν(CO) Transient Absorptions in Pure TCE and TCE + MeOH Solutions[a]

	TCE		TCE + 10% MeOH	
	ν(C═C)	ν(CO)	ν(C═C)	ν(CO)
		$\lambda_{ex} = 345$ nm		
A (cm^{-1})	12.0 ± 0.3	12.2 ± 0.4	12.3 ± 0.2	10.8 ± 0.3
τ (ps)	5.4 ± 0.4	10.9 ± 0.7 [a]	5.1 ± 0.2	3.8 ± 0.3
τ' (ps)	6.2 ± 0.3	6.0 ± 0.4	5.5 ± 0.2	2.8 ± 0.2
Γ (cm^{-1})	15.9 ± 0.3	14.5 ± 0.3	15.3 ± 0.2	15.8 ± 0.3
		$\lambda_{ex} = 400$ nm		
A (cm^{-1})	14.3 ± 0.2	22.7 ± 0.5	9.6 ± 0.2	13.4 ± 0.5
τ (ps)	7.3 ± 0.2	2.7 ± 0.1	4.4 ± 0.3	2.7 ± 0.3
τ' (ps)	8.6 ± 0.1	3.4 ± 0.1	5.9 ± 0.1	2.1 ± 0.2
Γ (cm^{-1})	15.3 ± 0.2	21.7 ± 0.2	13.6 ± 0.1	13.6 ± 0.3

[a] A and Γ are parameters defined by eq 1, and λ_{ex} corresponds to the excitation wavelength. Included are also characteristic times τ' obtained from exponential fits of the time dependent band positions (see Figure 9). [b] This number should be taken with caution due to large scatter in the data (see Figure 8a).

of the transient band when it is first formed, τ is the characteristic time at which the additional width decays, and IRF is the instrumental resolution of the spectral observation. In our analysis eq 1 is applied for the transient bands formed on the low-energy side of the CO and C═C stretching modes of the ground state of the Fe(acac)$_3$ molecule. The obtained parameters are shown in Table 2, and the corresponding fits to the line-narrowing data are shown in Figure 8.

The analysis shows rather consistently that the transient IR bands, after their prompt appearance within the initial excitation pulse, manifest vibrational cooling in the 3−9 ps time range. There is no evident solvent dependence of the relaxation times. The obtained cooling rates are consistent with those obtained for photochemically prepared products such as Rh(CO)(acac)-(n-hexane)[6] but are an order of magnitude faster than reported for Mn(CO)$_5$ being formed in the photolysis of Mn$_2$(CO)$_{10}$ in cyclohexane and isopropane.[9] For Fe(acac)$_3$, the fact that band narrowing of the transient absorptions is 2−5 times faster than bleach recovery, and that the time independent band maxima are still shifted by 2−11 cm^{-1} to the red with respect to the ground electronic state features, allows us to exclude vibrational cooling in the ground state as a possible candidate for the reported transient absorptions. Furthermore, the relatively small shift of the excited state vibrational absorptions from those of the ground state shows that the structural differences between these states are not substantial.[30] In fact, the relaxed transient absorptions can be associated with the fundamental vibrations of the bottleneck electronic state. These absorptions are at 1567−1574 and 1519−1522 cm^{-1} for ν(CO) and ν(CC), respectively. Consistent with this interpretation is the fact that once the bottleneck excited state is vibrationally relaxed (time independent line shape) the integrated absorption of the transient vibrations decay with a time constant similar to that of the bleach recovery. Noteworthy is that line-narrowing observed in the visible transient spectrum of Cr(acac)$_3$ was ascribed to vibrational cooling in the lowest energy electronic state, ^{2}E, in ∼1 ps time scale.[21] Also in this case, no significant spectral shift was observed between the electronic absorption spectra of the ground and lowest energy excited states, which is consistent with the intraconfigurational spin flip nature of the ^{2}E state.

The obtained time constants from the analysis of the bandwidths and band positions show some variation, which should be taken with caution. Because the line shape analysis contains some arbitrariness in the choice of parameters and the signals are relatively weak and they partially overlap with the bleach, small differences should not be considered reliable. However, in particular the data obtained in TCE at 400 nm excitation (see Figures 8b and 9b) show clearly different cooling rates for the ν(CO) and ν(CC) modes. The difference appears consistently in both analyses. In principle, such behavior requires that during relaxation, vibrational energy is not statistically distributed among the internal degrees of freedom. Although it is generally accepted that in large molecules vibrational energy redistribution occurs statistically, the energy flow cannot be infinitely fast. In the solution phase, strong intermolecular couplings may efficiently compete with intramolecular couplings and, consequently, relaxation may show mode selective behavior. In fact, this type of behavior has been observed in several studies.[31−33] The initial excitation of different vibrational modes is determined by the Franck−Condon factors associated with electronic coupling between different modes. The observed broadening and shift of the transient bands depend on the coupling strength of the mode, which is observed, with all the excited modes. If the rate of intermolecular energy transfer (IET) is mode specific and greater than the rate of intramolecular vibrational energy redistribution (IVR), two modes of different nature can show unequal cooling rates. The data shown in Figures 8 and 9, and Table 2 indicate this type of behavior for the ν(CO) and ν(CC) modes of Fe(acac)$_3$. However, because the total relaxation may include contribution from multiple electronic conversions, in addition to IET and IVR, the physics behind the present observations may be more complex. Although additional experiments are clearly needed to resolve full dynamics of the system, the present data could, indeed, indicate mode selectivity in vibrational cooling.

Rigorous description of the observed dynamics of Fe(acac)$_3$ would necessitate detailed knowledge of the various potential energy surfaces possibly involved in the relaxation chain from the initial excitation to the final recovery of the ground state molecule. Unfortunately, due to the complexity of its electronic structure, such information is not available for Fe(acac)$_3$. The analysis of the vis/UV pump−vis probe study on Cr(acac)$_3$ is used to aid the interpretation of the present transient IR data. As a d^5 system, the atomic energy levels of Fe are split in a dense manifold of ligand field states in octahedral symmetry, and these states are accompanied by MLCT and LMCT states, as well as excited states of the ligands. Some of the electronic configurations are sketched in Figure 10. The ground state of Fe(acac)$_3$ is ^{6}A$_1$ and has a very low transition probability to other ligand field components, and no evidence of such transitions is seen in Figure 3. Excitation at 345 and 400 nm is ascribed to MLCT and LMCT transitions,[25] respectively.

Excitation within the ^{4}LMCT band of Cr(acac)$_3$ leads to conversion to the ligand field ^{2}E state in time scale of ∼50 fs.[21] The ^{2}E state shows vibrational cooling on a time scale of ∼1 ps and eventually populates the ground state in the 700 ps time scale.[21] Because Fe(acac)$_3$ is the d^5 analogue of Cr(acac)$_3$, it is tempting to suggest that it might have somewhat similar relaxation dynamics. This would mean that the initial charge transfer excitation of either ^{4}LMCT at 400 nm or ^{4}MLCT at 345 nm is converted fast to some of the ligand field states, which have sufficient lifetime to support vibrational cooling before final conversion to the ground state. Again, analogously with the chromium compound, the spin flip states ^{4}E and ^{4}A$_1$ are the most probable candidates for such states. To make this consistent with the experimental observations, the lifetimes of the spin flip states of Fe should be significantly shorter than their counterpart in Cr. An alternative explanation for the observed transient bands is that they belong to the charge

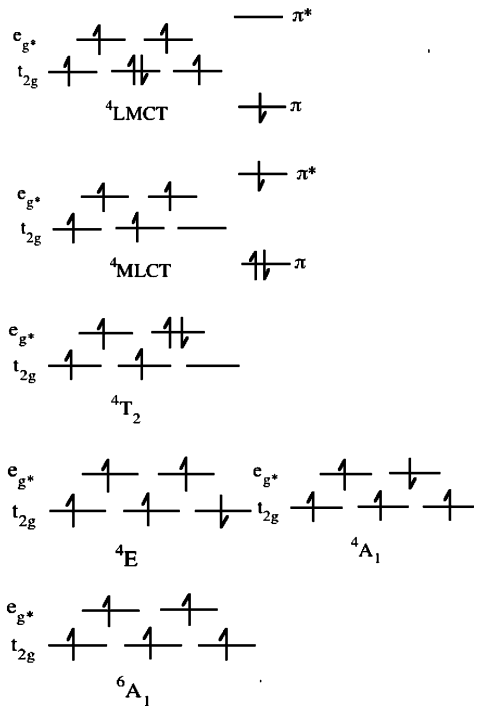

Figure 10. Schematic representation of some of the electronic configurations of $Fe(acac)_3$ in one electron representation. The superscripts of the charge transfer states indicate the number of unpaired electrons in the metal.

transfer states being excited by the 400 or 345 nm pulses. This would mean that, in contrast with the Cr compound, these states are decoupled from the ligand field manifold and relax directly to the ground state in ~10 ps time scale. However, the fact that the excited state IR absorptions are less than 11 cm^{-1} red-shifted with respect to the ground state bands provides a relatively solid argument against this mechanism. The charge transfer states involve either removal of an electron from a bonding orbital of the ligand or addition of an electron to an antibonding orbital. In both cases there should be a marked change in the bond order, which would, in turn, significantly affect the force constants of the vibration. Indeed, on the basis of electronic structure calculations on the isolated ligand, the estimated shifts in band position for both the MLCT and LMCT states are higher than 60 cm^{-1}, leading to a spectral signature in the probed region completely different from that of the observed transients.[34]

Conclusions

The ultrafast dynamics of $Fe(acac)_3$ has been studied by exciting the MLCT and LMCT charge transfer states by UV pulses at 345 and 400 nm, respectively, and monitoring the transient behavior of the system by IR spectroscopy in the 1600−1500 cm^{-1} region. It is shown that both excitation wavelengths lead to efficient bleach of the ground state molecule on a time scale limited by instrumental response time. The bleach recovers with a characteristic time of 8−19 ps depending on the excitation wavelength and the solvent. The fastest recovery times were obtained in binary TCE + MeOH solution. The complete recovery of the bleached absorptions in 50−60 ps indicates that $Fe(acac)_3$ is resistant to photoinduced ligand substitution by the solvent; moreover, its relaxation is not affected by long-lived electronic states, as reported for $Cr(acac)_3$.[21] Parallel with the decrease of the ν(CO) and ν(C═C) absorption intensities, new bands appeared on their low-energy side. The bandwidths and positions of these transient absorptions were observed to have strong time dependence, which was assigned to vibrational cooling with characteristic time of 3−9 ps. The most plausible interpretation of the experimental observation is that electronic conversion from the charge transfer states being excited by the triggering pulse to the ligand field manifold occurs within a few picosecods and produces a vibrationally hot electronically excited state. This state differs from the ground state most probably by a spin flip. Interestingly, comparison of time evolution of the ν(CO) and ν(C═C) transient absorptions of the spin flip state indicate mode specific vibrational cooling dynamics. Finally, electronic conversion to the ground state proceeds with a time constant of 8−15 ps. In an effort to further resolve the relaxation mechanism of $Fe(acac)_3$, we are now planning UV pump−vis probe experiments. A deeper understanding of the electronic structure from theoretical calculations would also greatly benefit interpretation of the excited state dynamics.

Acknowledgment. We thank professor Peter Hamm (University of Zürich) for his kind help in constructing our transient IR spectrometer. Professor Reijo Sillanpää (University of Jyväskylä) is thanked for suggesting $Fe(acac)_3$ as our first target in ultrafast IR spectroscopy and providing the substance. E.M. acknowledges the European Commission for Marie Curie Intra-European Fellowship, and M.P. acknowledges the Academy of Finland for financial support.

References and Notes

(1) Zewail, A. H. *Science* **1998**, *242*, 1988.
(2) Assmann, J.; Kling, M.; Abel, B. *Angew. Chem., Int. Ed.* **2003**, *42*, 2226.
(3) Mantz, J.; Wöste, L. E. *Femtosecond Chemistry*; VCH: New York, 1995.
(4) De Schrywer, F. C.; De Feyter, S.; Schweitzer, G. *Femtochemistry*; Wiley-VCH: Weinheim, 2001.
(5) Nibbering, E. T. J.; Fidder, H.; Pines, E. *Annu. Rev. Phys. Chem.* **2005**, *56*, 337.
(6) Dougherty, T. P.; Grubbs, W. T.; Heilweil, E. J. *J. Phys. Chem.* **1994**, *98*, 9396.
(7) Snee, P. T.; Payne, C. K.; Mebane, S. D.; Kotz, K. T.; Harris, C. B. *J. Am. Chem. Soc.* **2001**, *123*, 6909.
(8) Asplund, M. C.; Snee, P. T.; Yeston, J. S.; Wilkens, M. J.; Payne, C. K.; Yang, H.; Kotz, K. T.; Frei, H.; Bergman, R. G.; Harris, C. B. *J. Am. Chem. Soc.* **2002**, *124*, 10605.
(9) Steinhurst, D. A.; Baronavski, A. P.; Owrutsky, J. C. *Chem. Phys. Lett.* **2002**, *361*, 513.
(10) Lehtovuori, V.; Aumanen, J.; Myllyperkiö, P.; Rini, M.; Nibbering, E, T. J.; Korppi-Tommola, J. *J. Chem. Phys. A* **2004**, *108*, 1644.
(11) Schanz, R.; Bolan, V.; Hamm, P. *J. Chem. Phys.* **2005**, *122*, 044509.
(12) Lindner, J.; Vöhringer, P.; Pshenichnikov, M. S.; Cringus, D.; Wiersma, D. A.; Mostovoy, M. *Chem. Phys. Lett.* **2006**, *421*, 329.
(13) Shanoski. J. E.; Payne, C. K.; Kling, M. F.; Glascoe, E. A.; Harris, C. B. *Organometallics* **2005**, *24*, 1852.
(14) Glascoe, E. A.; Kling, M. F.; Shanoski, J. E.; Harris, C. B. *Organometallics* **2006**, *25*, 775.
(15) Shanoski, J. E.; Glascoe, E. A.; Harris, C. B. *J. Phys. Chem. B* **2006**, *110*, 996.
(16) Yang, H.; Snee, P. T.; Kotz, K. T.; Payne, C. K.; Harris, C. B. *J. Am. Chem. Soc.* **2001**, *123*, 4204.
(17) Grubbs, W. T.; Heilweil, E. J. *J. Chem. Phys.* **1994**, *100*, 4006.
(18) Owrutsky, J. C.; Baronavski, A. P. *J. Chem. Phys.* **1996**, *105*, 9864.
(19) Gumbel, G.; Elias, H. *Inorg. Chim. Acta* **2003**, *342*, 97.
(20) Diaz-Acosta, I.; Baker, J.; Cordes, W.; Pulay, P. *J. Phys. Chem. A* **2001**, *105*, 238.
(21) Juban, E. A.; McCusker, J. K. *J. Am. Chem. Soc.* **2005**, *127*, 6857.
(22) Dunne, T. G.; Cotton, F. A. *Inorg. Chem.* **1963**, *2*, 263.
(23) Bredenbeck, J.; Hamm, P. *Rev. Sci. Instrum.* **2003**, *74*, 3188.
(24) Hamm, P.; Kaidl, R. A.; Stenger, J. *Opt. Lett.* **2000**, *25*, 1798.
(25) Lintvedt, R. L.; Kernitsky, L. K. *Inorg. Chem.* **1970**, *9*, 491.
(26) Zinato, E.; Riccieri, P.; Sheridan, P. S. *Inorg. Chem.* **1979**, *18*, 720.
(27) Monat, J. E.; McCusker, J. K. *J. Am. Chem. Soc.* **2000**, *122*, 4092.
(28) Bhasikuttan, A. C.; Suzuki, M.; Nakashima, S.; Okada, T. *J. Am. Chem. Soc.* **2002**, *124*, 8398.

(29) Hamm, P. *Chem. Phys.* **1995**, *200*, 415.
(30) The small shift in the vibrational stretching frequencies indicates relatively minor structural differences between the ground and excited states with respect to these coordinates. There is likely to be a very large structural change along other coordinates (e.g., the Fe-O distance).
(31) Hogiu, W.; Werncke, W.; Pfeiffer, M.; Elsaesser, T. *Chem. Phys. Lett.* **1999**, *321*, 407.
(32) Elles, C. G.; Bingemann, D.; Heckscher, M. M.; Crim, F. F. *J. Chem. Phys.* **2003**, *118*, 5587.
(33) Sando, G. M.; Zhong, Q.; Owrutsky, J. C. *J. Chem. Phys.* **2004**, *121*, 2159.
(34) Ab initio calculations of vibrational frequencies were performed at the MP2/6-31G(d,p) level on the optimized structures calculated at the MP2/cc-pVDZ level.